

NASA
TP
1586
c.1

NASA Technical Paper 1586

THIS COPY RETURN TO
AFWL TECHNICAL LIBRARY
KIRTLAND AFB, NM

Baroclinic Instability With Variable Gravity - A Perturbation Analysis



Albert C. Giere, William W. Fowles,
and Salvador Arias

JANUARY 1980

NASA



NASA Technical Paper 1586

Baroclinic Instability With Variable Gravity - A Perturbation Analysis

Albert C. Giere, William W. Fowlis,
and Salvador Arias
*George C. Marshall Space Flight Center
Marshall Space Flight Center, Alabama*



National Aeronautics
and Space Administration

**Scientific and Technical
Information Office**

1980

TABLE OF CONTENTS

	Page
I. INTRODUCTION	1
II. FORMULATION OF THE PROBLEM	3
III. SOLUTION BY A PERTURBATION METHOD	7
IV. DISCUSSION.	18
REFERENCES	23

LIST OF ILLUSTRATIONS

Figure	Title	Page
1.	Distribution of gravity, $g/g_0 = 1 - \mu z$ for the values of μ as indicated.	8
2.	Distribution of the rotational Froude number, $F/F_0 = 1 + \mu z$, for the values of μ as indicated	8
3.	Distribution of the zonal flow, $\delta^{-1}u = z - \frac{1}{2}\mu z^2$ for the values of μ as indicated	9
4.	Variation of the phase speed, c_r , for $\delta = 1$, with the wavenumber κ for the values of μ as indicated	15
5.	Variation of the normalized growth rate, κc_i , for $\delta = 1$, with the wavenumber κ for the values of μ as indicated	16
6.	Variation of the phase speed, c_r , for $\delta = (1 - \mu/2)^{-1}$, with the wavenumber $\bar{\kappa}$ for the values of μ as indicated	19
7.	Variation of the normalized growth rate, $\bar{\kappa} c_i$, for $\delta = (1 - \mu/2)^{-1}$, with the wavenumber $\bar{\kappa}$ for the values of μ as indicated	20

BAROCLINIC INSTABILITY WITH VARIABLE GRAVITY — A PERTURBATION ANALYSIS

I. INTRODUCTION

When the Space Shuttle becomes operational in the 1980's, some of the flights will take into orbit a laboratory known as Spacelab. Spacelab will have the environment of a laboratory on the Earth's surface, except that when in orbit the value of effective gravity will be very small. A principal use of Spacelab will be to exploit this low gravity environment for science and technology. In particular, it will be possible to perform geophysical fluid flow model experiments in true spherical geometry. A radial dielectric body force, which is analogous to gravity, can be achieved over a volume of liquid held between two spheres. Such experiments cannot be performed in a laboratory on the Earth's surface because the dielectric body force cannot be made large enough to dominate the effect of terrestrial gravity. A spherical model of the baroclinic, synoptic-scale processes of the Earth's atmospheric circulation is being designed for Spacelab.

Since the last century, laboratory investigations seeking insight into large-scale circulations of the Earth's atmosphere have been performed. In these experiments a fluid was subjected to a horizontal temperature gradient and rotation; the temperature gradient modeled the polar-equatorial gradient and the rotation of the fluid container modeled the rotation of the Earth. The early experiments were qualitative in nature; systematic and quantitative developments date from the 1950's. Experiments in rotating cylindrical containers with heating at the rim and cooling at the base were carried out by Fultz et al. (1959). These experiments established the existence of two flow regimes, an axisymmetric flow for high heating and low rotation and an unsteady, non-axisymmetric flow for low heating and high rotation. Experiments in a rotating cylindrical annulus with differential radial heating were performed by Hide (1958), who discovered a steady, non-axisymmetric flow regime in which a jet flow meandered in a regular manner between the boundary cylinders. These annulus wave flows proved more amenable to systematic study than the cylinder flows (Fultz et al., 1959; Fowles and Hide, 1965; Kaiser, 1970).

Scaling of the governing equations for the large-scale features for both the atmosphere and the laboratory models leads to a set of approximate equations for both systems (Holton, 1972). These equations are known as the quasi-geostrophic equations. Thus, the experiments are models of the synoptic-scale atmospheric flow. It is generally agreed that baroclinic instability is the process responsible for the large-scale, nonaxisymmetric flow in both the atmosphere and the models (Lorenz, 1962).

Although much has been learned from the cylindrical annulus experiments, further progress is inhibited by the geometrical difference between the cylindrical annulus and the Earth's thin, spherical-shell atmosphere. The obstacle to the extension of the cylindrical experiments to spherical geometry has been the difficulty of simulating a dominant radial body force. For a dielectric liquid contained between two concentric spheres and subject to a voltage difference across the spheres in the manner of a spherical capacitor, it has been shown by Hart (1976) that a radial dielectric body force of the following form exists:

$$g_E = \frac{2\epsilon_o \eta}{\rho_o \gamma} \left(\frac{R_o R_i}{R_o - R_i} \right) \frac{V^2}{r^5}, \quad (1)$$

where R_i and R_o are the radii of the inner and outer spheres, respectively; ϵ_o and ρ_o are the dielectric constant and the density, respectively, at some reference temperature; η and γ are the temperature coefficients of dielectric constant and density, respectively; V is the voltage difference; and r is any radius between R_i and R_o . Values for the dimensions of the proposed Spacelab experiment and for the properties of suitable dielectric oils yield a typical value of $g_E = 200 \text{ cm/sec}^2$ (Hart, 1976; Fowlis and Fichtl, 1977). Thus, the need to perform these spherical model experiments onboard Spacelab becomes clear. Only in a low gravity environment will the dielectric body force dominate.

The fact that effective Spacelab gravity will not be exactly zero is due to orientation rocket firings, crew movements, the vibration of Shuttle and Spacelab equipment, gravity gradient oscillations of the Shuttle, the deceleration in orbit due to atmospheric drag, etc. The combined effect of these sources will depend on many variables, but a typical value is estimated at 0.1 cm/sec^2 , which gives a ratio of 5×10^{-4} when compared to the value of the dielectric body force previously given. For special "quiescent" orbital flight periods, this ratio could be several orders of magnitude smaller.

Design calculations are in progress for a spherical, baroclinically unstable model for Spacelab. Ultimately, a numerical, nonlinear, spherical model will be constructed, but to achieve understanding many theoretical calculations of increasing complexity have been undertaken. Since some of these calculations are also relevant to a wide range of research interests in theoretical dynamical meteorology and oceanography, they have been presented in publications (Fowlis and Arias, 1978; Geisler and Fowlis, 1979).

Equation (1) shows that the dielectric body force is a strong function of the radius. It was decided to calculate the effect of this variation on baroclinic instability. In Section II a quasi-geostrophic, baroclinic instability problem in which gravity is a function of height is formulated. In Section III a solution is obtained using a perturbation procedure. In Section IV the results are discussed and the relevant information for the design of the Spacelab experiment is presented. The solutions are also relevant to other geophysical fluid flows in which gravity is constant but the static stability is a function of height.

II. FORMULATION OF THE PROBLEM

The quasi-geostrophic equations used to formulate the stability problem are well known and will not be re-derived here. Systematic derivations and discussions have been given by Pedlosky (1964) and Holton (1972). We consider the fluid to be contained in a rotating rectilinear channel with rigid horizontal and vertical boundaries. The horizontal radial and zonal directions are denoted by x and y , respectively, and z denotes the vertical direction. The nondimensional, linearized, incompressible, quasi-geostrophic equation for the perturbation pressure, $p(x,y,z,t)$ is

$$\left(\frac{\partial}{\partial t} + u \frac{\partial}{\partial x} \right) \left\{ \nabla^2 p + \frac{\partial}{\partial z} \left(F \frac{\partial p}{\partial z} \right) \right\} + \frac{\partial q}{\partial y} \frac{\partial p}{\partial x} = 0 \quad , \quad (2)$$

where $u(y,z)$ is the basic state zonal flow velocity in the x -direction and $\partial q/\partial y$ is the meridional gradient of the potential vorticity of the basic state defined by

$$\frac{\partial q}{\partial y} = \beta - \frac{\partial}{\partial z} \left(F \frac{\partial u}{\partial z} \right) - \frac{\partial^2 u}{\partial y^2} \quad . \quad (3)$$

$F(z)$ is the rotational Froude number (inverse Burger number) defined by $F = f^2 L^2 / N^2 H^2$, where f is twice the rotation rate, and L and H are the respective distances between the boundaries in the y and z directions.

$N(z)$ is the Brunt-Vaisala frequency defined by $N = (\gamma g \partial T / \partial z)^{1/2}$, where g is the acceleration of gravity and $\partial T(y,z)/\partial z$ is the basic state vertical temperature gradient. The quantity β represents the scaled latitudinal derivative of f .

The nondimensional boundary conditions, which state that the normal component of flow at the boundaries is zero, are

$$\left(\frac{\partial}{\partial t} + u \frac{\partial}{\partial x} \right) \frac{\partial p}{\partial z} - \frac{\partial u}{\partial z} \frac{\partial p}{\partial x} = 0, \quad \text{on } z = 0, 1, \quad (4)$$

$$p = 0, \quad \text{on } y = 0, 1. \quad (5)$$

For a normal mode wave disturbance of the form

$$p = \text{Re} \{ \psi(y, z) \exp i k(x - ct) \}, \quad (6)$$

where $\psi(y, z)$ is the perturbed pressure, k is the zonal wave number (taken as real), and c is the phase speed (taken as complex, $c = c_r + ic_i$); equations (2), (4), and (5) become, respectively,

$$(u - c) \left\{ (F\psi_z)_z + \psi_{yy} - k^2 \psi \right\} + q_y \psi = 0, \quad (7)$$

$$(u - c) \psi_z - u_z \psi = 0, \quad \text{on } z = 0, 1, \quad (8)$$

$$\psi = 0, \quad \text{on } y = 0, 1, \quad (9)$$

where the suffixes denote differentiation.

To solve the problem we take u as a function of z only and put $\beta = 0$. Equation (7) then takes the form

$$(u - c) \left\{ (F\psi_z)_z + \psi_{yy} - k^2 \psi \right\} - (Fu_z)_z \psi = 0. \quad (10)$$

Equation (10) is separable. Assuming a solution of the form $\psi(y, z) = \chi(y) \phi(z)$ and using the boundary conditions (9), we obtain

$$\psi(y, z) = \phi(z) \sin m\pi y, \quad (11)$$

$$(u - c) \left\{ (F\phi_z)_z - K^2\phi \right\} - (Fu_z)_z \phi = 0 \quad , \quad (12)$$

where $K^2 = k^2 + m^2\pi^2$, $m = 1, 2, \dots$. The boundary conditions (8) become

$$(u - c) \phi_z - u_z \phi = 0 \quad , \quad \text{on } z = 0, 1 \quad . \quad (13)$$

We are concerned with the solution of equation (12) for variable gravity. For a general power law, equation (1) can be written in the form

$$g = g_0 \left(1 + \frac{Hz}{z_0} \right)^{-n} \quad , \quad (14)$$

where g_0 and z_0 are values at the origin of the coordinates and n is a constant. Using equation (14) and assuming that all other quantities in F are independent of z , we obtain

$$F(z) = F_0 \left(1 + \frac{Hz}{z_0} \right)^n \quad , \quad (15)$$

where $F_0 = f^2 L^2 / N_0^2 H^2$ and $N_0 = (\gamma g_0 \partial T / \partial z)^{1/2}$ and where F_0 and N_0 are independent of z . From the thermal wind relationship, we have for the dimensional vertical shear of the basic state

$$U_z(z) = \frac{g\gamma}{f} \frac{\partial T}{\partial y} \quad .$$

Using equation (14) and again assuming that all other quantities are independent of z , we obtain

$$u_z(z) = \zeta_0 \zeta_\mu^{-1} \left(1 + \frac{Hz}{z_0} \right)^{-n} \quad , \quad (16)$$

where $\zeta_0 = g_0 \gamma f^{-1} \partial T / \partial y$ and ζ_μ is a characteristic value of $U_z(z)$ used to nondimensionalize $U_z(z)$. ζ_0 and ζ_μ are independent of z . Let us consider the last term in equation (12). Note, using equations (15) and (16), that the combination $F u_z$ is independent of z , and hence this term vanishes identically. Equation (12) then reduces to

$$(F \phi_z)_z - K^2 \phi = 0 \quad . \quad (17)$$

Expanding equations (14), (15), and (16) to first-order in μ , we obtain

$$g = g_0 (1 - \mu z) \quad (18)$$

$$F = F_0 (1 + \mu z) \quad (19)$$

$$\delta^{-1} u_z = (1 - \mu z) \quad , \quad (20)$$

where $\mu = nH/z_0$ and $\delta = \zeta_0 \zeta_\mu^{-1}$. Integrating equation (20) from $z = 0$ to z we obtain

$$\delta^{-1} u = (z - \frac{1}{2} \mu z^2) \quad . \quad (21)$$

Equations (18) through (21) approximate the more exact forms previously given when μ is small. In the next section we shall solve this approximate variable g problem.

The solution of the problem for constant g , (i.e. $\mu = 0$) was first given by Eady (1949). A succinct statement of Eady's problem has been given by McIntyre (1970). Eady's problem is formulated from the above equations as

$$\phi_{ozz} - \kappa^2 \phi_0 = 0 \quad , \quad (22)$$

$$(u_0 - c_0) \phi_z - u_{oz} \phi_0 = 0 \quad , \quad \text{on } z = 0, 1, \quad (23)$$

$$u_0 = z \quad , \quad (24)$$

where $\kappa = K/F_0^{1/2}$. The solutions are

$$c_0 = \frac{1}{2} \pm \frac{1}{2} \alpha^{-1} \{(\alpha - \coth \alpha)(\alpha - \tanh \alpha)\}^{1/2} \quad , \quad (25)$$

$$\phi_0 = \kappa c_0 \cosh \kappa z - \sinh \kappa z \quad , \quad (26)$$

where $\alpha = \kappa/2$. The solutions represent either an amplifying-decaying pair of waves with $c_r = R_e(c_0) = 1/2$, or a pair of neutral waves with $c_r \geq$ and $\leq 1/2$, according as $\kappa <$ or $\geq \kappa_N$, where

$$\kappa_N = 2.3994 \quad (\kappa_N = \coth \kappa_N) \quad . \quad (27)$$

There is a short wavelength cutoff to the instability at the critical neutral wavenumber κ_N . There is also a maximum growth rate for some $\kappa < \kappa_N$; $\kappa = \kappa_M$.

III. SOLUTION BY A PERTURBATION METHOD

In this section we shall solve the problem posed by equations (17), (18), (19), (13), and (21) using a perturbation method. The procedure followed is that described by McIntyre (1970) and it requires that $\mu \ll 1$. Figures 1, 2, and 3 show g/g_0 , F/F_0 , and $\delta^{-1}u$ from equations (18), (19), and (21), respectively, plotted as functions of z for $\mu = 0, 0.05, 0.1, 0.3$ and 0.5 . We take μ to be a perturbation parameter and write

$$F(z)/F_0 = 1 + \mu F_1(z) \quad , \quad (28)$$

$$\delta^{-1}u(z) = z + \mu u_1(z) \quad , \quad (29)$$

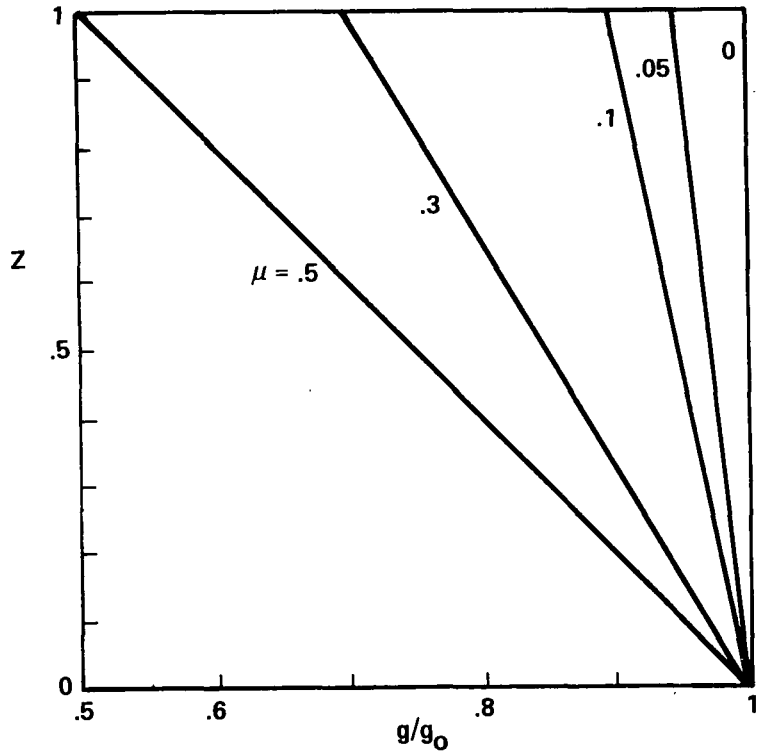


Figure 1. Distribution of gravity, $g/g_0 = 1 - \mu z$ for the values of μ as indicated.

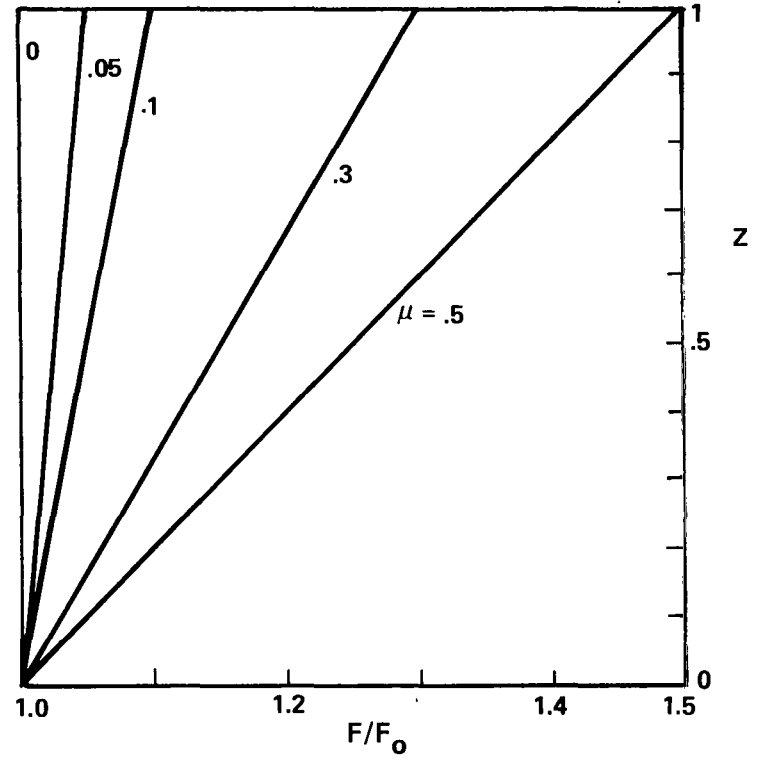


Figure 2. Distribution of the rotational Froude number, $F/F_0 = 1 + \mu z$, for the values of μ as indicated.

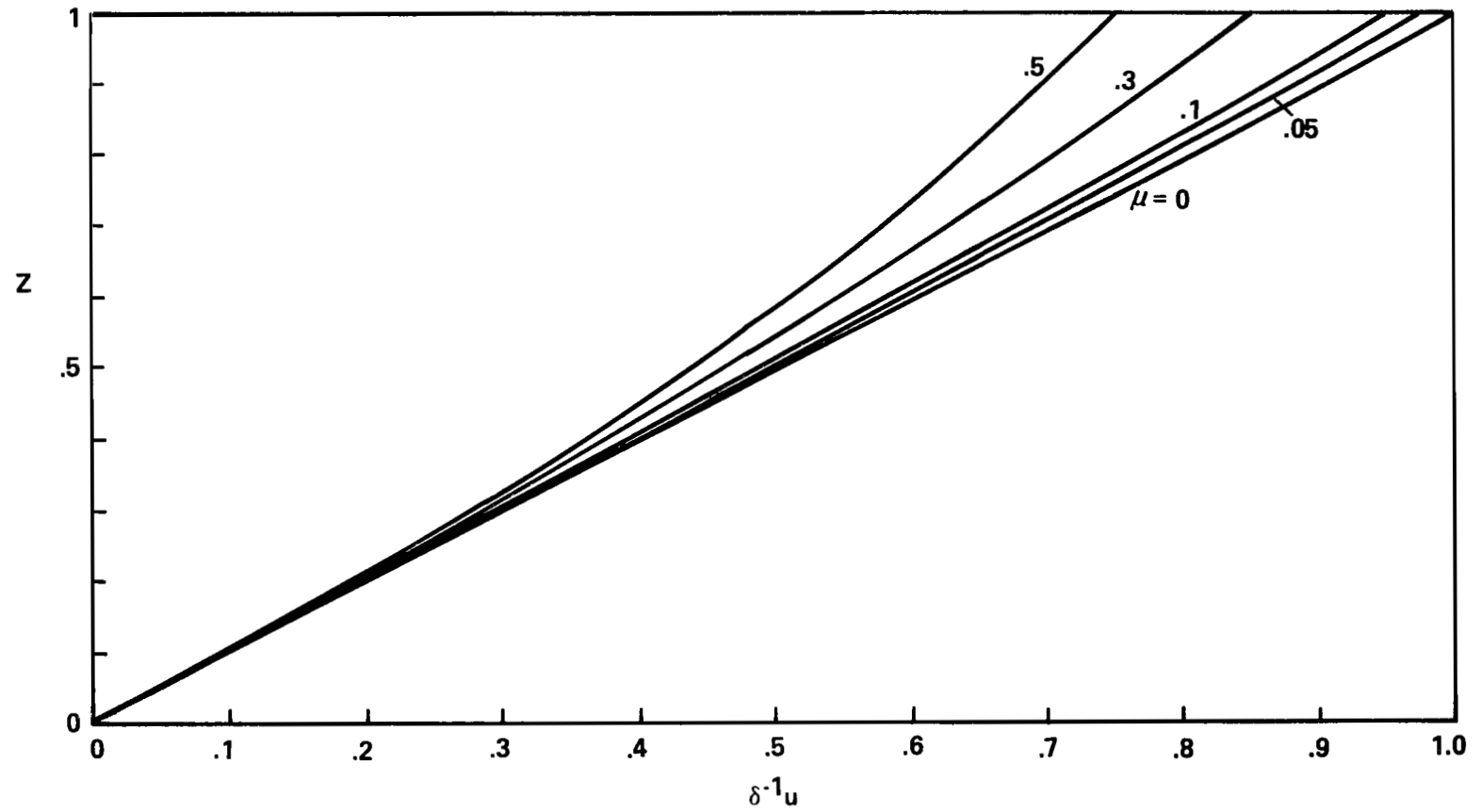


Figure 3. Distribution of the zonal flow, $\delta^{-1}u = z - \frac{1}{2} \mu z^2$ for the values of μ as indicated.

where

$$F_1(z) = z \quad , \quad (30)$$

and

$$u_1(z) = -\frac{1}{2} z^2 \quad . \quad (31)$$

The method is to expand $\phi(z)$ and c about the Eady solutions (see Section II) in the following way

$$\phi = \phi_0 + \mu \phi_1 + \mu^2 \phi_2 + \dots \quad , \quad (32)$$

$$c = c_0 + \mu c_1 + \mu^2 c_2 + \dots \quad . \quad (33)$$

It turns out that this expansion, in integral powers of μ , is appropriate only for the case $\kappa \neq \kappa_N$, where κ_N is the transition wave-number from the neutral wave regime to the unstable wave regime. For the case $\kappa = \kappa_N$, the correction terms obtained from the expansions (32) and (33) diverge. This is because the Eady solutions possess branch points at $\kappa = \kappa_N$. In view of this, two separate cases will be considered. For the first case $\kappa \neq \kappa_N$, the appropriate expansions are (32) and (33). For $\kappa = \kappa_N$, an expansion in powers of $\mu^{1/2}$ has been found to be appropriate, namely

$$\phi = \phi_0 + \mu^{1/2} \phi_1 + \mu \phi_2 + \dots \quad , \quad (34)$$

$$c = c_0 + \mu^{1/2} c_1 + \mu c_2 + \dots \quad . \quad (35)$$

The substitution of equations (28) and (32) into equation (17) yields, to zero and first-order in μ , respectively

$$\phi_{0zz} - \kappa^2 \phi_0 = 0 \quad , \quad (36)$$

$$\phi_{1zz} - \kappa^2 \phi_1 = -\frac{F_{1z}}{F_0} \phi_{0z} - \frac{F_1}{F_0} \phi_{0zz} \quad , \quad (37)$$

where $\kappa = K/F_0^{1/2}$. With the aid of equation (36), equation (37) becomes

$$\phi_{1zz} - \kappa^2 \phi_1 = -\frac{F_{1z}}{F_0} \phi_{0z} - \frac{F_1}{F_0} \kappa^2 \phi_0 \quad . \quad (38)$$

In a similar fashion, the substitution of equations (29), (32), and (33) into the boundary conditions (13) yields, to zero and first-order, respectively

$$(z - \tilde{c}_0) \phi_{0z} - \phi_0 = 0 \quad , \quad \text{on } z = 0, 1 \quad , \quad (39)$$

$$(z - \tilde{c}_0) \phi_{1z} - \phi_1 + (u_1 - \tilde{c}_1) \phi_{0z} - u_{1z} \phi_0 = 0 \quad , \quad z = 0, 1 \quad , \quad (40)$$

where $\tilde{c}_0 = \delta^{-1} c_0$ and $\tilde{c}_1 = \delta^{-1} c_1$. Combining these two equations, we obtain

$$(z - \tilde{c}_0) \phi_{1z} - \phi_1 + \left(\frac{u_1 - \tilde{c}_1}{z - \tilde{c}_0} - u_{1z} \right) \phi_0 = 0 \quad , \quad \text{on } z = 0, 1 \quad . \quad (41)$$

Substituting from equations (30) and (31) into equations (38) and (41), we have finally

$$\phi_{1zz} - \kappa^2 \phi_1 = -\phi_{0z} - \kappa^2 z \phi_0 \quad , \quad (42)$$

$$(z - \tilde{c}_0) \phi_{1z} - \phi_1 - \left[\frac{z_1^2 + 2\tilde{c}_1}{2(z - \tilde{c}_0)} - z \right] \phi_0 = 0, \text{ on } z = 0, 1. \quad (43)$$

It can easily be shown that the general solution of the non-homogeneous equation (42) is

$$\phi_1 = \frac{1}{4} (\kappa^2 z^2 + 3\tilde{c}_0 \kappa z + A) \cosh \kappa z - (\tilde{c}_0 \kappa^2 z + 3z + B) \sinh \kappa z, \quad (44)$$

which is the first-order correction to the eigenfunctions. With the aid of the boundary conditions (43), the two constants A and B can be reduced to one arbitrary constant. Our primary interest, however, is the determination of the first-order correction to the eigenvalue c .

We multiply equation (42) by ϕ_0 and integrate from $z = 0$ to $z = 1$. The first term on the left is integrated by parts twice, and then, with the aid of (36), we obtain the result

$$\phi_0 \phi_{1z} \Big|_0^1 - \phi_{0z} \phi_1 \Big|_0^1 = -\kappa^2 \int_0^1 z \phi_0^2 dz - \frac{1}{2} \phi_0^2 \Big|_0^1. \quad (45)$$

From the zero and first-order boundary conditions, equations (39) and (40), we find

$$\begin{aligned} \phi_{0z}(0) &= -\frac{\phi_0(0)}{\tilde{c}_0}, \\ \phi_{0z}(1) &= \frac{\phi_0(1)}{1 - \tilde{c}_0}, \\ \phi_{1z}(0) &= \frac{\tilde{c}_1}{2\tilde{c}_0} \phi_0(0) - \frac{\phi_1(0)}{\tilde{c}_0}, \end{aligned}$$

$$\phi_{1z}(1) = \frac{1}{2(1 - \tilde{c}_0)^2} [(2\tilde{c}_1 + 2\tilde{c}_0 - 1) \phi_0(1) + 2(1 - \tilde{c}_0) \phi_1(1)] .$$

Substituting these into equation (45), simplifying and solving for \tilde{c}_1 , we obtain

$$\tilde{c}_1 = \frac{-\tilde{c}_0^2}{2[\tilde{c}_0^2 \phi_0^2(1) - (1 - \tilde{c}_0)^2 \phi_0^2(0)]} \left\{ \frac{\tilde{c}_0^2}{2} + 2\kappa^2(1 - \tilde{c}_0^2) \int_0^1 z \phi_0^2(z) dz \right\} . \quad (46)$$

With the aid of the Eady eigenfunctions (26), this expression for \tilde{c}_1 can be expressed in terms of hyperbolic functions. A neat form can be derived by eliminating the hyperbolic functions using identities derivable from equation (25). After some substantial and judicious algebraic manipulation, it can be shown that

$$\tilde{c}_1 = \frac{(1 - \tilde{c}_0)^2 (\tilde{c}_0^2 \kappa^2 - 1)}{4(1 - 2\tilde{c}_0)} - \frac{\tilde{c}_0^2}{4} . \quad (47)$$

Equation (47) involves only the unperturbed eigenvalue \tilde{c}_0 . We note that if \tilde{c}_0 is real, \tilde{c}_1 is real. If \tilde{c}_0 is complex, the real and imaginary parts of \tilde{c}_1 , are given by

$$\tilde{c}_{1r} = \frac{1}{16\alpha^2} (R^2 - 3\alpha^2) , \quad (48)$$

$$\tilde{c}_{1i} = \pm \frac{1}{16\alpha R} [(\alpha^2 + R^2) - \alpha^2 - R^2] , \quad (49)$$

where $R^2 = -(\alpha - \coth \alpha)(\alpha - \tanh \alpha)$ and $\alpha = \kappa/2$. For \tilde{c}_0 real, \tilde{c}_1 is given by

$$\tilde{c}_{1r} = -\frac{1}{16\alpha^2} (S^2 + 3\alpha^2) \pm \frac{1}{16\alpha S} [(\alpha^2 - S^2) - (\alpha^2 - S^2)^2] , \quad (50)$$

$$\tilde{c}_{1i} = 0 ,$$

where $S^2 = -R^2$. Thus, for $\alpha < \coth \alpha$, ($\kappa < \kappa_N$) we have finally,

$$c_r = \frac{\delta}{2} + \frac{\mu \delta}{16\alpha^2} (R^2 - 3\alpha^2) , \quad (51)$$

$$c_i = \pm \delta \left\{ \frac{R}{2\alpha} + \frac{\mu}{16\alpha R} [(\alpha^2 - R^2) - (\alpha^2 - R^2)^2] \right\} , \quad (52)$$

and for $\alpha > \coth \alpha$, ($\kappa > \kappa_N$),

$$c_r = \frac{\delta}{2} - \frac{\mu \delta}{16\alpha^2} (S^2 + 3\alpha^2) \pm \delta \left\{ \frac{S}{2\alpha} + \frac{\mu}{16\alpha S} [(\alpha^2 - S^2) - (\alpha^2 - S^2)^2] \right\} , \quad (53)$$

$$c_i = 0 . \quad (54)$$

The quantity $\delta (= \zeta_0 \zeta_\mu^{-1})$ depends on a characteristic value for $U_z(z)$. We shall first plot the results for $\zeta_\mu = \zeta_0$, and hence for $\delta = 1$. This means that for the characteristic value of ζ_μ we have chosen the single representative value at $z = 0$. Figure 4 shows the phase speeds calculated from equations (51) and (53) and plotted as c_r versus κ for $\mu = 0.1, 0.3$ and 0.5 . The Eady result (see Section II) corresponding to $\mu = 0$ is also shown. Figure 5 shows the growth rates calculated from equations (52) and (54) and plotted as κc_i versus κ for $\mu = 0, 0.1, 0.3$ and 0.5 . Note that the values diverge as the wave number approaches the Eady critical value $\kappa = \kappa_N = 2.3994$.

As was discussed earlier in this section, the expansions (34) and (35) must be used at $\kappa = \kappa_N$. Following the general procedure used above for $\kappa \neq \kappa_N$, it can be shown that for $\kappa = \kappa_N$

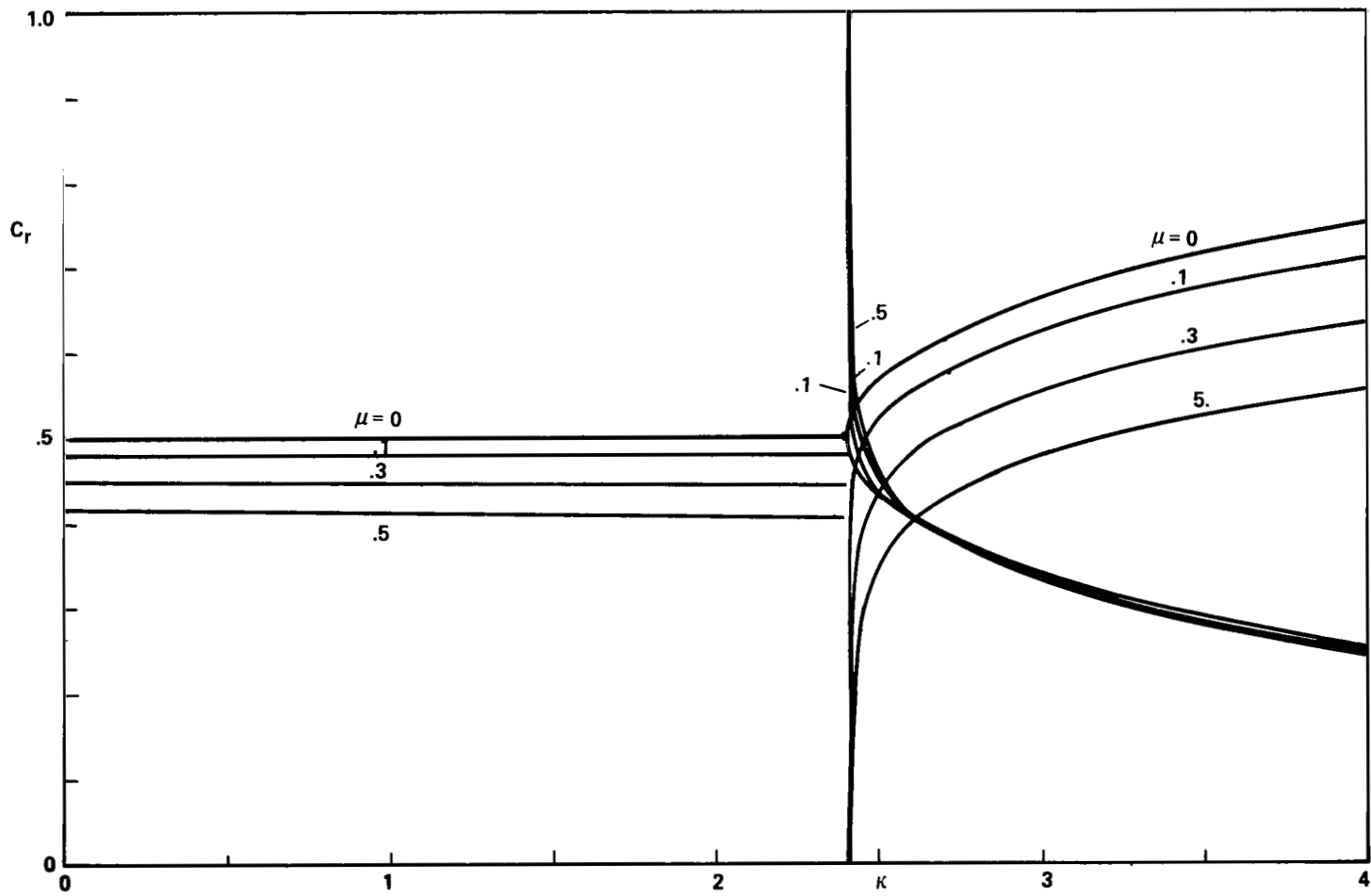


Figure 4. Variation of the phase speed, c_r , for $\delta = 1$, with the wavenumber κ for the values of μ as indicated.

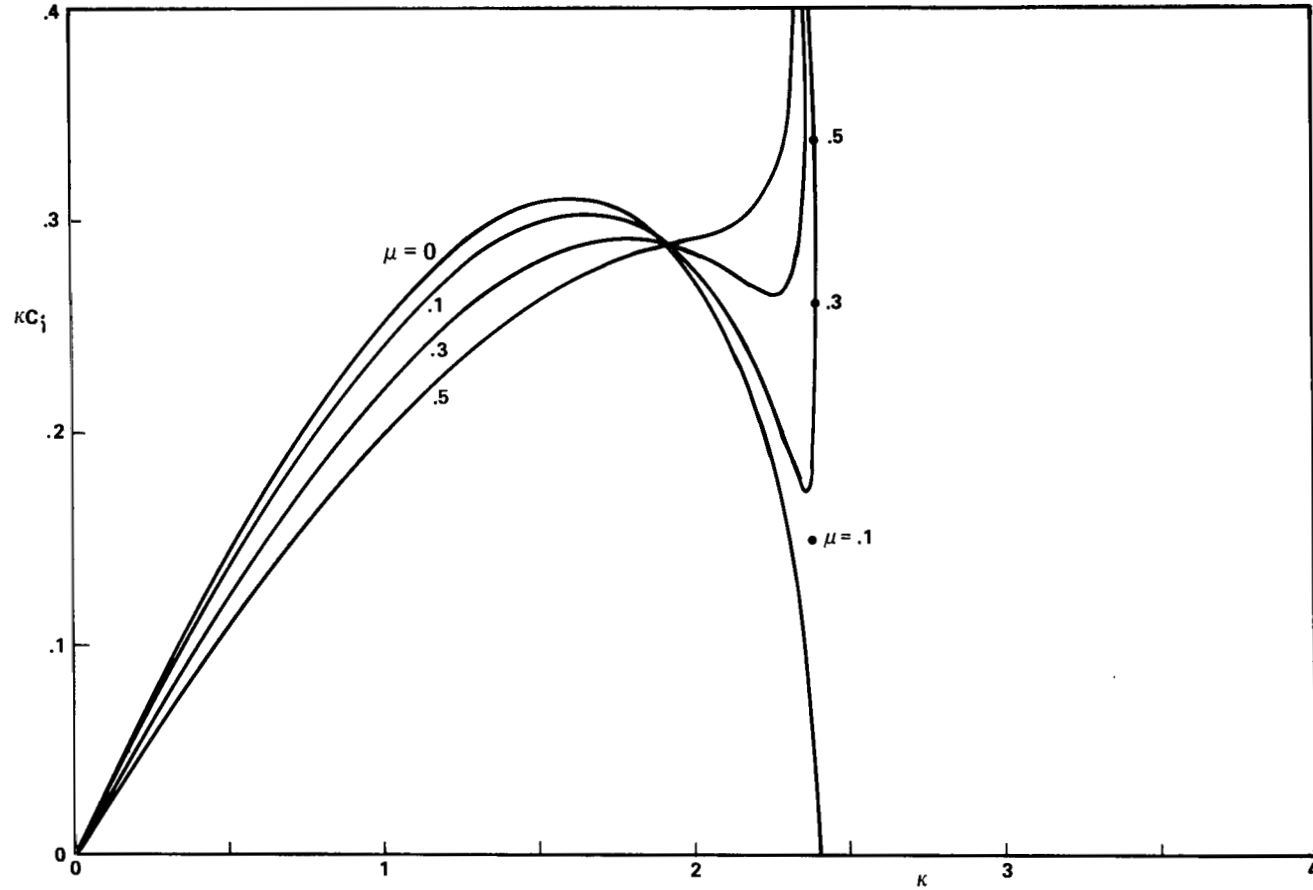


Figure 5. Variation of the normalized growth rate, κC_i , for $\delta = 1$, with the wavenumber κ for the values of μ as indicated.

$$\tilde{c}_0 = \frac{1}{2} , \quad (55)$$

$$\tilde{c}_1 = \pm i \frac{\kappa_N (\kappa_N^2 - 4)^{1/2}}{16} . \quad (56)$$

Thus, we have

$$c_r = \frac{\delta}{2} , \quad (57)$$

$$c_i = \pm \mu^{1/2} \delta \frac{\kappa_N (\kappa_N^2 - 4)^{1/2}}{16} . \quad (58)$$

These results are shown as dots in Figures 4 and 5 for $\delta = 1$ and for the same values of μ as the curves already plotted.

The plots in Figures 4 and 5 are based on representative values of F and u_z at $z = 0$. This means that they show the effects of both an average lower value for g as well as the variation of g , whereas plots based on characteristic average values of F and u_z would show only the consequences of the variation of g . Let us choose linear averages over z for F and u_z , defined by

$$\bar{F} = \int_0^1 F(z) dz$$

and

$$\delta_\mu = \int_0^1 u_z(z) dz .$$

Substitution from equations (19) and (20), respectively, and performing the simple integrations, we obtain

$$\bar{F} = 1 + \frac{\mu}{2} , \quad \text{implying that} \quad \kappa = \bar{\kappa} \left(1 + \frac{1}{2} \mu\right)^{1/2} , \quad (59)$$

$$\delta = \left(1 - \frac{1}{2} \mu\right)^{-1} . \quad (60)$$

Figures 6 and 7 present plots of the phase speed and growth rates based on equations (51) and (53), and (52) and (54), respectively, and using equations (59) and (60). The dots are based on equations (57) and (58) and using (59) and (60).

Since only the first-order corrections are calculated, the results are accurate only for small μ . The results should be reasonably valid for $\mu = 0.1$, but for the larger values of μ moderate errors are certainly present.

IV. DISCUSSION

In this paper we formulated an approximate, quasi-geostrophic, baroclinic stability problem for a body force with a height dependence. The primary motivation for this work was to determine the effect of a variable dielectric body force, analogous to gravity, on baroclinic instability for the design of a spherical, atmospheric, synoptic-scale model experiment for Spacelab. In the formulation, curvature and horizontal shear of the basic state were omitted and the vertical and horizontal temperature gradients of the basic state were taken as constants independent of z . A consequence of the body force variation and the above assumptions is that the transverse gradient of the potential vorticity of the basic state vanishes. This stability problem was then solved using a perturbation method.

Figure 5 shows the well known results due to Eady ($\mu = 0$), that for $\kappa = \kappa_N = 2.3994$, unstable waves exist, and for $\kappa > \kappa_N$ neutral waves exist (see Section II). The growth rates for the non-zero values of μ are qualitatively similar to Eady's results and converge to Eady's result as $\mu \rightarrow 0$. Note that, because of the divergent behavior at $\kappa = \kappa_N$, we cannot accurately locate the critical value of κ for each value of μ . However, by extrapolation using the point values, we can see that the critical values move to larger values of κ as μ increases. Figure 5 shows that in general the growth rates decrease as μ increases. This is not surprising since a dimensional statement shows the growth rate depends linearly on g , and g decreases as μ increases. Note the cross-over point to the right of which the opposite is true.

Figure 4 shows that the phase speed of the unstable mode decreases as μ increases and is only weakly dependent on κ . Using equation (21) we obtain for the average value of $\delta^{-1}u$, $\delta^{-1}\bar{u} = 1/2 - \mu/6$.

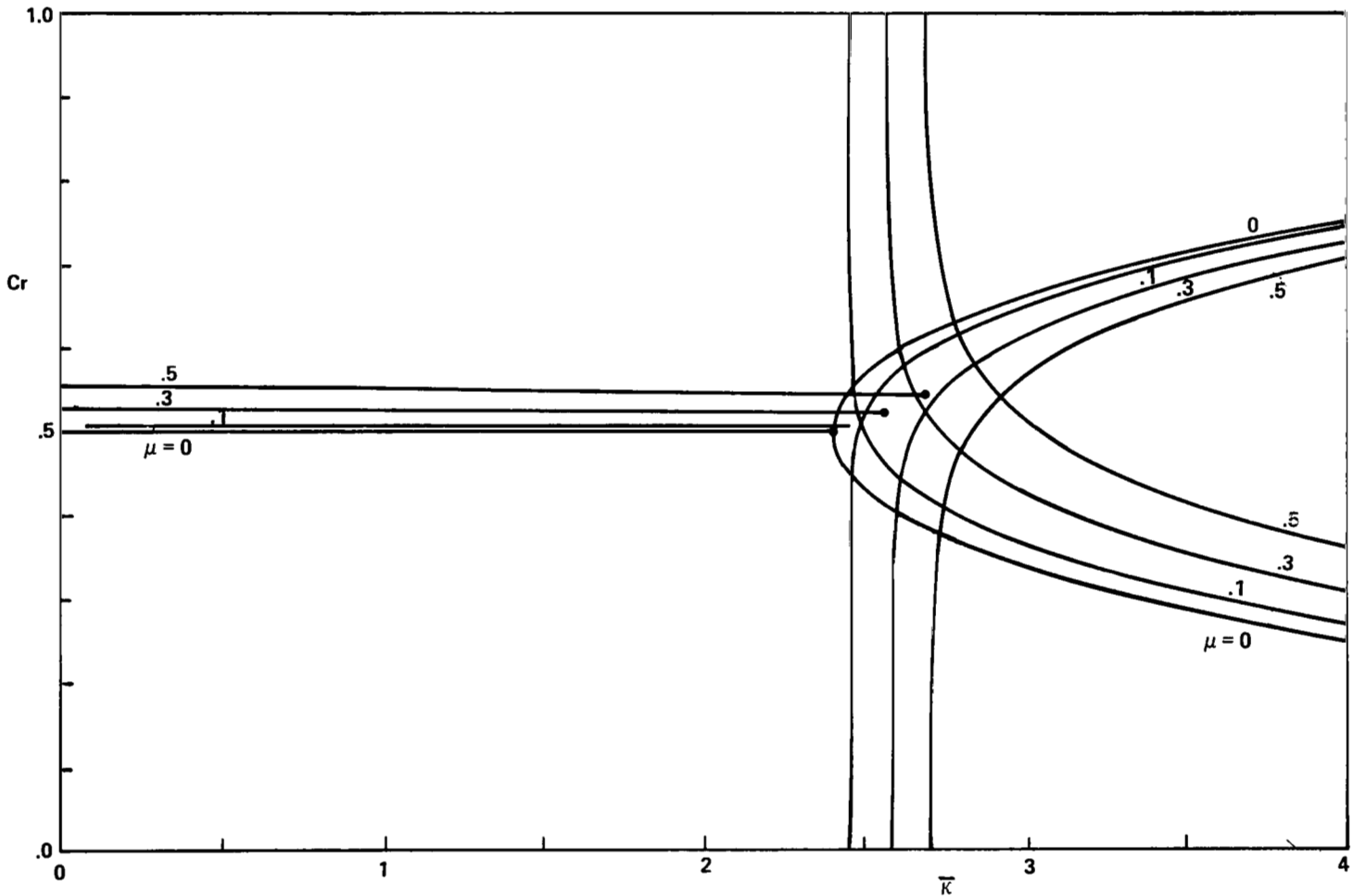


Figure 6. Variation of the phase speed, c_r , for $\delta = (1 - \mu/2)^{-1}$, with the wavenumber \bar{k} for the values of μ as indicated.

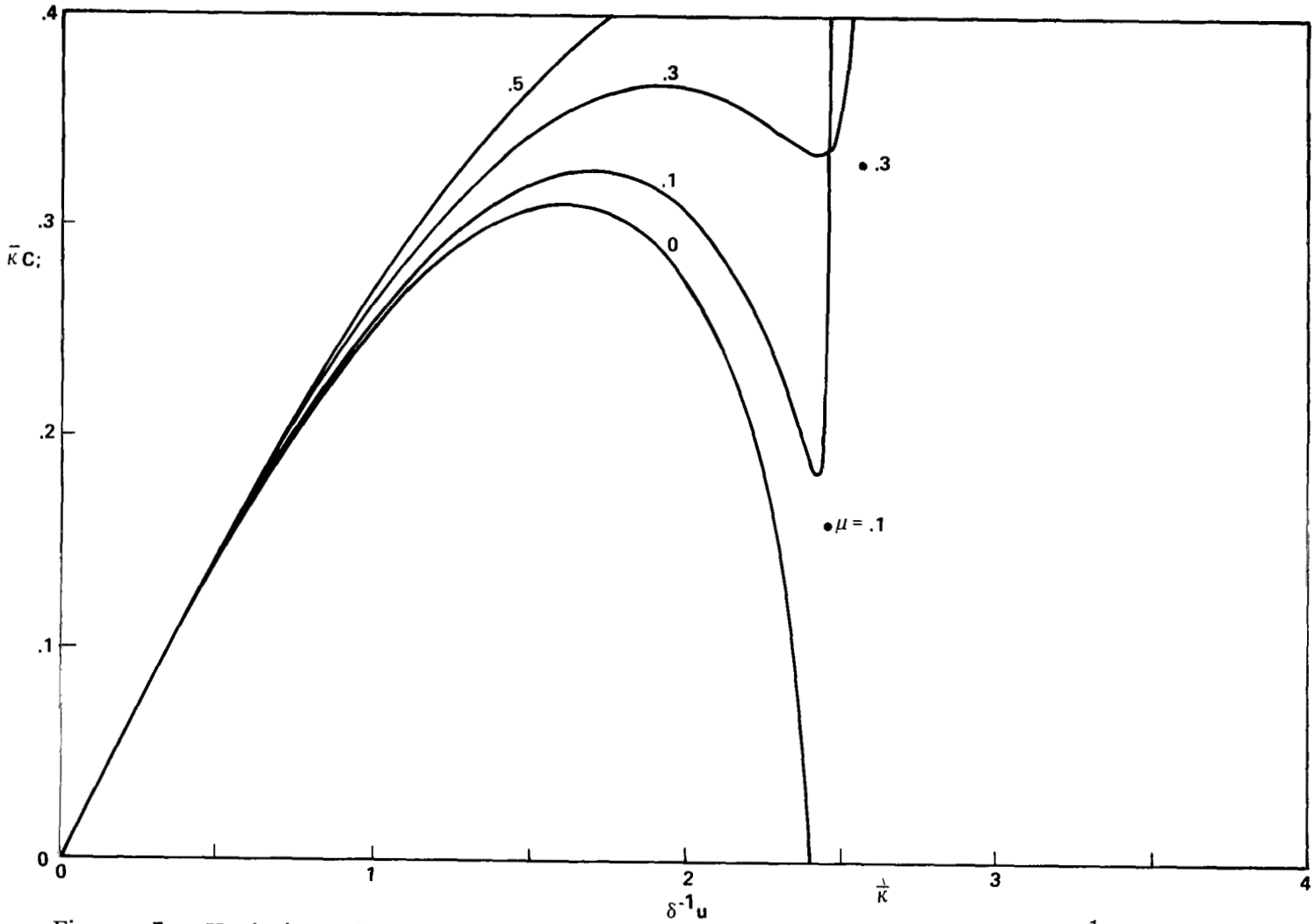


Figure 7. Variation of the normalized growth rate, $\bar{\kappa}c_i$, for $\delta = (1 - \mu/2)^{-1}$, with the wavenumber $\bar{\kappa}$ for the values of μ as indicated.

For $\delta = 1$ and $\mu = 0.1, 0.3$ and 0.5 , $\bar{u} = 0.483, 0.450$ and 0.417 , respectively. The phase speeds are in good agreement with these values. Thus, like the Eady result, the unstable mode is simply advected at the rate of the mean flow. The levels at which the actual flow corresponds to the phase speed of the unstable wave are known as the steering levels, and are found by solving

$$z_s - \frac{1}{2} \mu z_s^2 = \frac{1}{2} - \frac{\mu}{6} .$$

In the stable region there are two neutral modes, one confined near the upper boundary and one near the lower boundary (Bretherton, 1966; Hyun and Fowles, 1979). Each of these neutral modes also propagates with a phase speed related to a mean flow in its environment. The phase speed of the lower mode does not vary much as a function of μ since the basic flow does not change much in the lower region (Fig. 3). However, in the upper region there is a substantial change as a function of μ in the flow, and this is reflected in the phase speed.

Figures 6 and 7 show the phase speeds and growth rates plotted in terms of averaged values of the basic state. For small values of $\frac{\bar{\kappa}}{\kappa}$ the growth rates are now almost independent of μ but for values of $\frac{\bar{\kappa}}{\kappa}$ near the maximum growth rate and near the critical values, the growth rates are larger.

We now proceed to ascertain what information the calculation has for the design of the Spacelab experiment. For this experiment, $n = 5$ [see equation (1)] and the gap-to-mean-radius ratio, H/z_0 , will be approximately 0.1. Thus $\mu = nH/z_0 \approx 0.5$. Our first-order perturbation calculation cannot be expected to give an accurate answer for such a large value of μ , but an approximate result and the general behavior of the instability as g varies can be expected. [We should also remember that the binomial approximation was used to formulate the equations (18), (19) and (20) and the accuracy here depends again on μ being small.] The plots show that the results are qualitatively similar to Eady's results. No new phenomena have appeared. The growth rates based on averaged values are somewhat larger than for the Eady problem, and the range of instability is somewhat increased. Phase speeds remain close to mean flow speeds. Thus, the results suggest that for a body force variation of 50 percent, the stability characteristics are not much changed. Future design studies should treat this problem more accurately.

Although the effect of variable gravity on baroclinic instability, per se, is not of much value in understanding atmospheric and oceanic flows and laboratory geophysical fluid flow experiments, the solutions we

have obtained can be relevant to these flows. The variation in g which leads to a variation in the Brunt-Vaisala frequency, N , and in turn to a variation in the rotational Froude number, F , could formally have been due to a variation in the vertical temperature gradient, $\partial T/\partial z$, with g constant (see the definitions of N and F in Section II). Thus, if we deal with a flow for which N is a function of z and for which the vertical shear is also a function of z , such that the gradient of the potential vorticity, q_y , vanishes, then our solutions are relevant. The ocean and the laboratory cylindrical annulus (see Section I) are systems in which the static stability undergoes large variation with height.

REFERENCES

- Bretherton, F. P. (1966): Baroclinic Instability and the Short Wavelength Cut-Off in Terms of Potential Vorticity. *Quart. J. Roy. Met. Soc.*, 92, 335.
- Eady, E. T. (1949): Long Waves and Cyclone Waves. *Tellus*, 1, 33.
- Fowlis, W. W. and Arias, S. (1978): The Effects of Curvature and Viscosity on Baroclinic Instability — A Two-Layer Model. NASA Technical Paper 1328.
- Fowlis, W. W. and Fichtl, G. H. (1977): Geophysical Fluid Flow Model Experiments in Spherical Geometry. Proceedings of the Third NASA Weather and Climate Program Science Review. NASA Conference Publication 2029, Paper No. 32.
- Fowlis, W. W. and Hide, R. (1965): Thermal Convection in a Rotating Annulus of Liquid: Effects of Viscosity on the Transition Between Axisymmetric and Non-Axisymmetric Flow Regimes. *J. Atmos. Sci.*, 22, 541.
- Fultz, D., Long, R. R., Owens, G. V., Bohan, W., Kaylor, R., and Weil, J. (1959): Studies of Thermal Convection in a Rotating Cylinder with Some Implications for Large-Scale Atmospheric Motions. *Meteor. Monog.*, 4, No. 21, pp 104, Amer. Met. Soc., Boston, MA.
- Geisler, J. E. and Fowlis, W. W. (1979): Theoretical Regime Diagrams for Thermally Driven Flows in a Beta-Plane Channel. *J. Atmos. Sci.*, 36, 1530.
- Hart, J. E. (1976): Studies of Earth Simulation Experiments. NASA Contractor Report NASA-CR2753.
- Hide, R. (1958): An Experimental Study of Thermal Convection in a Rotating Liquid. *Phil. Trans. Roy. Soc. Lond. A*, 250, 441.
- Holton, J. R. (1972): An Introduction to Dynamic Meteorology. International Geophysics Series, Academic Press.
- Hyun, J. M. and Fowlis, W. W. (1979): The Wave Structures of the Eady Model of Baroclinic Instability. NASA Technical Paper. In preparation.
- Kaiser, J. A. C. (1970): Rotating Deep Annulus Convection. Part 2. Wave Instabilities, Vertical Stratification, and Associated Theories. *Tellus*, 22, 275.

REFERENCES (Concluded)


- Lorenz, E. N. (1953): A Proposed Explanation for the Existence of Two Regimes of Flow in a Rotating Symmetrically-Heated Cylindrical Vessel. *Fluid Models in Geophysics, Proc. 1st Sympos. on the Use of Models in Geophys. Fluid Dynamics*, Baltimore.
- McIntyre, M. E. (1970): On the Non-Separable Baroclinic Parallel Flow Instability Problem. *J. Fluid Mech.*, 40, 273.
- Pedlosky, J. (1964): The Stability of Currents in the Atmosphere and the Ocean: Part I. *J. Atmos. Sci.*, 21, 201.

APPROVAL


BAROCLINIC INSTABILITY WITH VARIABLE GRAVITY - A PERTURBATION ANALYSIS

By Albert C. Giere, William W. Fowlis, and Salvador Arias


The information in this report has been reviewed for technical content. Review of any information concerning Department of Defense or nuclear energy activities or programs has been made by the MSFC Security Classification Officer. This report, in its entirety, has been determined to be unclassified.



GEORGE H. FICHTL
Chief, Fluid Dynamics Branch



WILLIAM W. VAUGHAN
Chief, Atmospheric Sciences Division



CHARLES A. LUNDQUIST
Director, Space Sciences Laboratory

1. REPORT NO. NASA TP-1586		2. GOVERNMENT ACCESSION NO.		3. RECIPIENT'S CATALOG NO.	
4. TITLE AND SUBTITLE Baroclinic Instability with Variable Gravity - A Perturbation Analysis				5. REPORT DATE January 1980	
				6. PERFORMING ORGANIZATION CODE	
7. AUTHOR(S) Albert C. Giere,* William W. Fowlis, and Salvador Arias				8. PERFORMING ORGANIZATION REPORT #	
9. PERFORMING ORGANIZATION NAME AND ADDRESS George C. Marshall Space Flight Center Marshall Space Flight Center, Alabama 35812				10. WORK UNIT NO. M-293	
				11. CONTRACT OR GRANT NO.	
12. SPONSORING AGENCY NAME AND ADDRESS National Aeronautics and Space Administration Washington, D.C. 20546				13. TYPE OF REPORT & PERIOD COVERED Technical Paper	
				14. SPONSORING AGENCY CODE	
15. SUPPLEMENTARY NOTES Prepared by Space Sciences Laboratory, Science and Engineering *Universities Space Research Association Visiting Scientist					
16. ABSTRACT Solutions are obtained for a quasi-geostrophic baroclinic stability problem in which gravity is a function of height. Curvature and horizontal shear of the basic state flow are omitted and the vertical and horizontal temperature gradients of the basic state are taken as constant. The primary motivation for this work was to determine the effect of a variable dielectric body force, analogous to gravity, on baroclinic instability for the design of a spherical, baroclinic model for Spacelab. Such modeling cannot be performed in a laboratory on the Earth's surface because the body force cannot be made strong enough to dominate terrestrial gravity. A consequence of the body force variation and the preceding assumptions is that the potential vorticity gradient of the basic state vanishes. The problem is solved using a perturbation method. The solution gives results which are qualitatively similar to Eady's results for constant gravity; a short wavelength cutoff and a wavelength of maximum growth rate are observed. Based on averaged values of the basic state, both the wavelength range of the instability and the growth rate at maximum instability are increased. The conclusion is that the presence of the variable body force will not significantly alter the dynamics of the Spacelab experiment. The solutions are also relevant to other geophysical fluid flows where gravity is constant but the static stability or Brunt-Vaisala frequency is a function of height.					
17. KEY WORDS Baroclinic instability Meteorology Upper ocean Lower atmosphere			18. DISTRIBUTION STATEMENT Category 42		
19. SECURITY CLASSIF. (of this report) Unclassified		20. SECURITY CLASSIF. (of this page) Unclassified		21. NO. OF PAGES 29	22. PRICE \$4.00

National Aeronautics and
Space Administration

Washington, D.C.
20546

Official Business

Penalty for Private Use, \$300

THIRD-CLASS BULK RATE

Postage and Fees Paid
National Aeronautics and
Space Administration
NASA-451



15 1 10, E, 120379 S00903DS
DEPT OF THE AIR FORCE
AF WEAPONS LABORATORY
ATTN: TECHNICAL LIBRARY (SUL)
KIRTLAND AFB NM 87117

NASA

POSTMASTER: If Undeliverable (Section 158
Postal Manual) Do Not Return

S